

## Ring Resonators and Mach-Zehnder Interferometers based sensors in a Si<sub>3</sub>N<sub>4</sub> technology

G. Micó<sup>1</sup>, D. Pastor<sup>1</sup>, D. Domenech<sup>2</sup>, C. Dominguez<sup>3</sup> and P. Muñoz<sup>1,2</sup>

<sup>1</sup> Universitat Politècnica de València – iTEAM, C/ Camino de Vera s/n, Valencia 46022, Spain.

<sup>2</sup> VLC Photonics S.L., C/ Camino de Vera s/n, Valencia 46022, Spain.

<sup>3</sup> Institute of Microelectronics of Barcelona, IMB-CNM (CSIC), Bellaterra (Barcelona) 08193, Spain.

*We propose the design of Ring Resonators (RRs) and Mach-Zehnder Interferometers (MZIs) based sensors in Silicon Nitride (Si<sub>3</sub>N<sub>4</sub>) technology for estimating the absorbance coefficient of different substances. Both RRs and MZIs incorporate Spiral Waveguides (SWGs) of different lengths from 4 to 18 mm to perform analysis at different interaction distances and different concentrations.*

### Introduction

Integrated optic sensors are a hot topic of research due to their outstanding characteristics and multiple applications in environmental, security, process control, and biomedicine applications, among others [1]. These sensors are based on Photonic Integrated Circuits (PICs) which combine a considerable amount of components in a single chip, obtaining equivalent functionality to bulky discrete systems, with the advantage of mass manufacturing and economies of scale. Nowadays prototyping PICs is affordable thanks to Multi-Project Wafer (MPW) runs, where fabrication costs are shared by users. The expansion of PICs has contributed to the creation of new brokers and foundries, and vice versa. In this paper we report on proof-of-concept sensors on a Silicon Nitride (SiO<sub>2</sub>/Si<sub>3</sub>N<sub>4</sub>/SiO<sub>2</sub>) platform [2].

### Sensing architectures

The designed sensors are based on evanescent wave sensing. As it is known, the light propagating inside a waveguide is mostly confined in the core region, but depending on the index contrast of the waveguide, part of the light can be spread in the outer part (evanescent field). For evanescent sensing, the sample under study is placed in contact with the waveguide core what produces changes in 1) the effective refractive index of the guide and 2) the amplitude of the signal due to absorption losses. In this paper, we focus on the absorption study and, in order to test the possibilities of the technology, we have chosen well known sensing architectures such as Mach-Zehnder Interferometers (MZIs) and Ring Resonators (RRs). Figure 1 shows the measuring schemes of MZIs and RRs sensors of different path lengths to analyze the sample absorbance following the Beer-Lambert Law. This law is defined as  $A = \varepsilon \cdot C \cdot b$  which states that the Absorbance (A) is linearly dependent on the concentration (C) of the sample and the sensing path length (b).  $\varepsilon$  is the molar absorptivity of the sample and is usually given in units of M<sup>-1</sup>cm<sup>-1</sup>, where M is the molar concentration. Hence, analyzing the amplitude variations for different concentrations and sensing path lengths the absorption coefficient of the sample can be obtained.

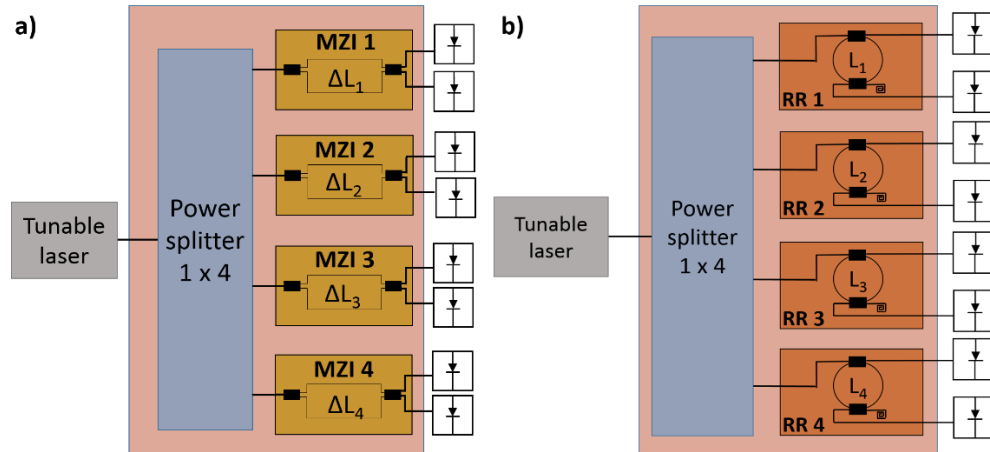


Figure 1. Measuring scheme of MZIs (a) and RRs (b) sensors to retrieve absorption information. In both cases two photo-detectors are used to obtain the response of the upper and lower output responses of the MZI, and transmission and reflection responses of the RR. For the target technology, the power splitter and the sensors (MZIs or RRs) may be on the same chip area.

To achieve higher sensitivity in the measurement, spiral waveguides have been implemented within the MZIs and RRs to increase the interaction paths (Figure 2). This technology allows selective area trenching, which means the removal of the cladding SiO<sub>2</sub> layer in selected zones [2]. These areas allow direct contact between the sample and evanescent field and they have been designed large enough to ensure a proper deposition of the sample.

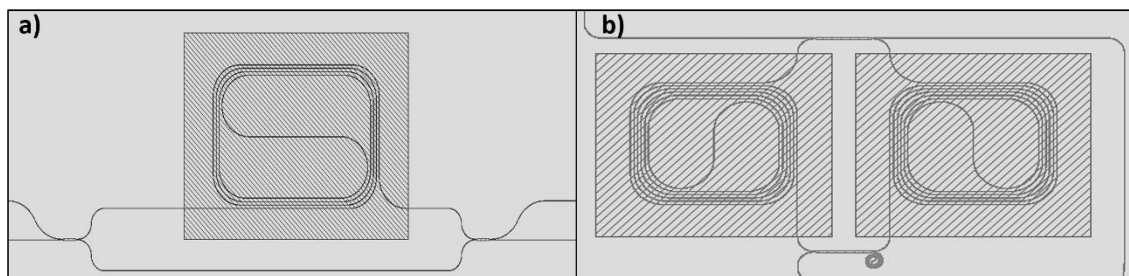


Figure 2. Layouts of a MZI (a) and a RR (b) using spirals to increase the interaction length of the sensors. Shaded areas correspond to trenched sections.

Regarding samples to study, we use aqueous solutions with different concentrations of Sodium Chloride (NaCl) and Glucose. Figure 3 shows the variation of refractive index ( $n$ ) and absorption coefficient ( $\alpha$ ) versus concentration. Both refractive index and absorption values depend on wavelength, concentration and temperature at which they are measured, i.e.  $N = N(\lambda, C, T)$ , where  $N$  is the complex refractive index. The real part of  $N$  is related with the refractive index while the complex part provides the extinction coefficient ( $\kappa$ ), which is associated with the absorption coefficient by the relation  $\alpha = 4\pi\kappa/\lambda$ . The values of Figure 3 plots are based on the literature [3-6] and are specific for 23°C temperature and 1550 nm wavelength.

We use these data to perform simulations and estimate the response of our sensors. First step is to define the cross-section of the waveguide (Figure 4) and obtain the values of the effective refractive index and propagation losses of the optical waveguide exposed to the solute. These simulations are performed using Phoenix Software and the PDK provided by the foundry. Solution material is configured to change its physical

properties determined by concentration, which is selected to shift between 0.1 – 1 M. Some values of  $n_{eff}$  and  $\alpha$  are shown in Table 1 where It can be appreciated the low propagation losses that presents the technology. Furthermore,  $\alpha$  values for both Glucose and NaCl solutions are shorter compare with literature ones, which is expected since exists low interaction light-sample in evanescent field sensing. Figure 4c shows the TE propagation mode inside the waveguide when a solution is placed on top of it.

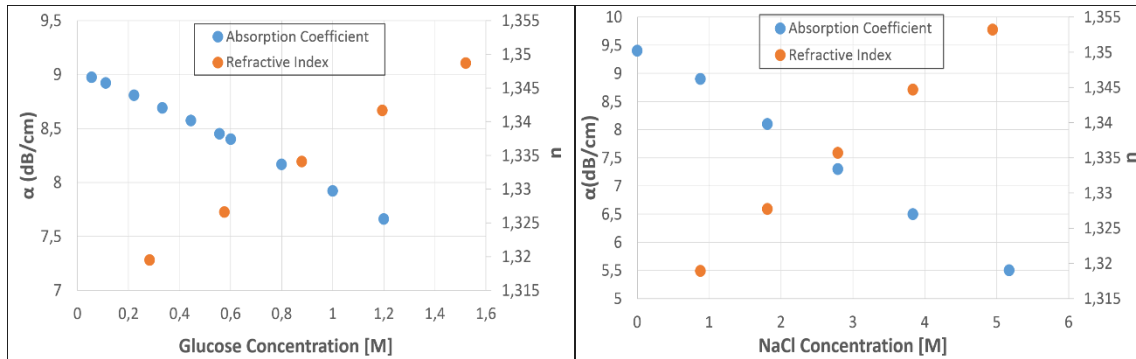


Figure 3. Representation of the absorption coefficient,  $\alpha$ , and the refractive index,  $n$ , of Glucose-Water (left) and NaCl-Water (right) solutions for different solute concentrations.



Fig. 4. Deeply etched waveguide cross-section with cladding (a) and trench (b). Section (c) shows the evanescent field propagating trough the trench area when a sample is deposited on it.

	$n_{eff}$	$\alpha$ (dB/cm)
Waveguide with cladding	1.5768	$1.979 \times 10^{-13}$
Waveguide with trench	1.5225	$2.325 \times 10^{-11}$
Glucose-Water solution in trench	1.5542	7.0121
NaCl-Water solution in trench	1.5531	7.1735

Table 1.  $n_{eff}$  and  $\alpha$  simulation values obtained at  $\lambda=1550$  nm and solute concentration in solution of 0.5M.

In the second step the effective indices found with the mode solver are used in Matlab to simulate the transfer function of the MZIs and RRs. The results are presented in Fig. 5, for different sensing path lengths at constant concentration. As we can see, there is a change in amplitude and also a shift in wavelength when the sample is placed in the trenched area. We could determine the value of  $n_{eff}$  by measuring the wavelength shift, but we would need to have a reference of the signal and knowing which cycle of the FSR we are analyzing. On the other hand, the absorbance coefficient of the sample can be obtained by evaluating the ratio between the minimum and maximum of the MZIs or RRs spectral transfer function, assuming the coupler behavior is ideal (in our case 50:50 power splitting). Nonetheless, the availability of two complementary outputs and

sensors with different sensing lengths may be used to cross-check and calibration methods measuring signals with and without solution in the trenched area.

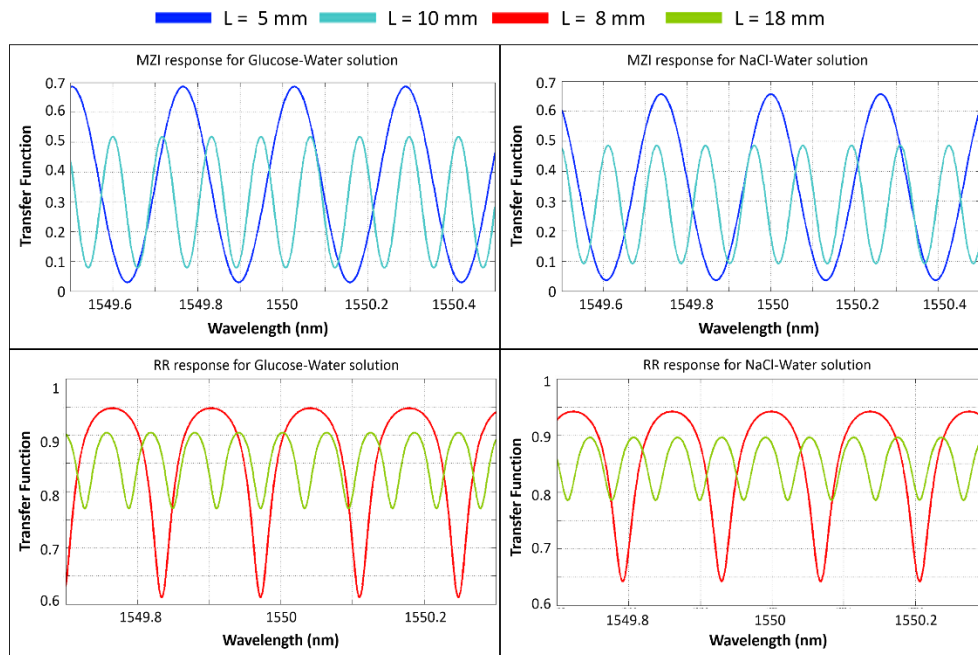


Fig.5. Transfer functions of MZIs (upper graphs) and RRs (lower graphs) based sensors for different sensing lengths at 0.5 M solute concentration.

## Conclusions

We have shown evanescent field sensors based on an innovative Si<sub>3</sub>N<sub>4</sub> technology. MZIs and RRs are designed to obtain the absorption coefficient of different solutions. Results from both sensor can be compare, although it is expected to get better sensitivity with RRs since light is in contact with the sample longer time. The employment of spiral waveguides within the devices makes possible to analyze substances of low absorption properties such as NaCl-Water solutions.

## Acknowledgements

This work is supported by the Spanish National MINECO under Project Ref. TEC2013-42332-P acronym “PIF4ESP”. G. Micó wishes to acknowledge FPI Grant BES-2014-068523.

## References

- [1] V.M.N. Passaro, C. de Tullio, B. Troia, M. la Notte, G. Giannoccaro and F. De Leonardis, “Recent Advances in Integrated Photonic Sensors”, *Sensors*, vol. 12, 15558-15598, 2012.
- [2] <http://www.vlcphotonics.com/>
- [3] H. Su and X.G. Huang, “Fresnel-reflection-based fiber sensor for on-line measurement of solute concentration in solutions”, *Sensors and Actuators B*, vol.126, 579-582, 2007.
- [4] R. Pan, J.B. Jeffries, T. Dreier and C. Schulz, “Measurements of liquid film thickness, concentration and temperature of aqueous NaCl solution by NIR absorption spectroscopy”, *Applied Physics B*, DOI 10.1007/s00340-015-6149-2
- [5] W. Zhang, R. Liu, W.Zhang, H. Jia and K. Xu, “Discussion on the validity of NIR spectral data in non-invasive blood glucose sensing”, *Biomedical Optics Express*, vol. 4, 789-802, 2013.
- [6] Jung Y., Hwang J., “Near-infrared studies of glucose and sucrose in aqueous solutions: water displacement effect and red shift in water absorption from water-solute interaction”, *Applied Spectroscopy*, vol. 67, 171-180, 2013.